JOURNAL OF SOLID STATE CHEMISTRY 60, 145–158 (1985)

An X-Ray and Neutron Powder Diffraction Study of the $Ca_{2+x}Nd_{8-x}(SiO_4)_6O_{2-0.5x}$ System[1]

J. A. FAHEY

Bronx Community College, Bronx, New York 10468

W. J. WEBER

Pacific Northwest Laboratory, Richland, Washington 99352

AND F. J. ROTELLA

Argonne National Laboratory, Argonne, Illinois 60439

Received November 2, 1984; in revised form April 22, 1985

The variation in lattice parameters with bulk composition and preparation temperature has been determined from X-ray powder diffraction data for the system $Ca_{2+x}Nd_{8-x}(SiO_4)_6O_{2-0.5x}$. The structures of two members of this system have been further refined from time-of-flight neutron powder diffraction data using the Rietveld method. Both structures belong to the $P6_3/m$ space group and are isomorphous with natural apatite, $Ca_{10}(PO_4)_6(F,OH)_2$. Samples prepared at 1250°C exhibit an ordered distribution of Ca and Nd cations between two nonequivalent sites. The room temperature lattice parameters of $Ca_2Nd_8(SiO_4)_6O_2$ are $a = 9.5291(5)$ Å and $c = 7.0222(1)$ Å, while those of $Ca_{2.2}Nd_{7.8}(SiO_4)_6O_{1.9}$ are $a = 9.5303(4)$ Å and $c = 7.0147(1)$ Å. The composition of the latter member is believed to represent the upper limit of solid solution for this system at 1250°C.

Introduction

The structure and stability of rare earth silicate isomorphs of natural apatite, $Ca_{10}(PO_4)_6(F,OH)_2$, are of interest in nuclear waste management because they can occur as actinide host phases in several high-level nuclear waste forms (*1–3*). The primary concern is the effect of alpha decay of the actinides, which can substitute for the rare earths in the crystal lattice, on both the structure and structure-related properties. Earlier studies (*1, 3*) of radiation effects in two simulated nuclear waste forms indicated that rare-earth silicates of this apatite structure type were unstable with respect to self-radiation and transformed from a crystalline to an essentially amorphous state. These observations prompted an extensive and ongoing investigation (*4, 5*) of radiation effects in the synthetic compound, $Ca_2Nd_8(SiO_4)_6O_2$, which was chosen because of its chemical and structural similarity to the rare-earth silicates observed in nuclear waste forms.

It was recognized early in the above study that a complete understanding of the

[1] Work supported by the U.S. Department of Energy under Contract DE-AC06-76RL0 1830.

0022-4596/85/$3.00

structure and stoichiometry limits of the $Ca_{2+x}Nd_{8-x}(SiO_4)_6O_{2-0.5x}$ system was necessary to fully understand and interpret the structural changes that accompany radiation damage. Consequently, another systematic study was also undertaken with the objective of obtaining a complete set of atomic coordinates and occupation factors for all atoms, along with solid solution limits, for this system. Prior to this study, the structure had only been inferred from the hexagonal symmetry revealed by its X-ray diffraction pattern, and the range of solid solution in the oxygen-deficient structure had been assumed to be very broad, extending to $x = 4$ (*6*). The initial structure refinement of the $Ca_{2+x}Nd_{8-x}(SiO_4)_6O_{2-0.5x}$ system, which has been previously reported (*7*), was carried out using powder X-ray diffraction data and a slightly modified version of the Rietveld–Hewatt profile analysis program (*8*). The results of that study showed that the structure (space group: $P6_3/m$) was indeed isostructural with natural apatite (*9*). In addition, both atomic coordinates and occupation factors were determined, and an upper compositional limit of $x = 1$ at 1250°C and $x = 0$ at 1600°C was suggested for this system. Additional work to more fully define the compositional limit was subsequently undertaken, and time-of-flight neutron powder diffraction studies have been carried out to further refine and verify the structure and stoichiometry limits. The results of these additional studies are reported in this paper.

Experimental

Specimen Preparation

In order to evaluate the extent to which calcium substitutes for neodymium in the generic compound, samples of different compositions were prepared. All preparations were carried out by dissolving appropriate amounts of Nd_2O_3 (99.99%) and CaO (99.9%) in 35% nitric acid and adding the resulting solution to an ammonia stabilized silicate solution containing the desired amount of SiO_2. (Note: The calcium oxide was heated to 1000°C to decompose any hydroxide or carbonate before weighing.) The solutions were evaporated to dryness, heated to 500°C for 2 hr to decompose nitrates to oxides, pressed into pellets, and fired at 1250°C for 24 hr. The resulting samples covered the composition range from $x = 0$ to 2.0, with x being the compositional variable of the system. (Our previous study (*7*) included a sample at $x = 4.0$, but that composition exhibited a glass-like calcium silicate phase in addition to the crystalline apatite phase.) A second set of samples for the same composition range was prepared from a portion of the first set of samples by crushing selected pellets, repressing into pellets, and then refiring at 1600°C for 24 hr. After cooling at 250°C/hr, the samples were crushed and ground in an agate mortar to less than 45-μm particle size for X-ray and neutron powder diffraction analysis.

X-Ray Diffraction

Powder X-ray diffraction patterns in the present study were obtained using two 114-mm Debye–Scherrer cameras. Calibration of each camera against NBS silicon powder ($a = 5.43088$ Å) resulted in an average experimental lattice parameter for silicon of 5.4308 (*2*) Å. The data for each sample were corrected for film shrinkage and the lattice parameters were refined using the program of Williams (*10*).

Neutron Measurements

Neutron irradiation and diffraction measurements were carried out at the Intense Pulsed Neutron Source (IPNS) Facility operated by Argonne National Laboratory. A description of the operation of pulsed neu-

TABLE I

SUMMARY OF THE RIETVELD ANALYSIS FOR $Ca_{2+x}Nd_{8-x}(SiO_4)_6O_{2-0.5x}$

	$Ca_2Nd_8(SiO_4)_6O_2$	$Ca_{2.2}Nd_{7.8}(SiO_4)_6O_{1.9}$
Crystal system	Hexagonal	Hexagonal
Crystal class	6/*m*	6/*m*
Space group	$P6_3/m$ (No. 176)	$P6_3/m$ (No. 176)
a (Å)	9.5291(5)	9.5303(4)
c (Å)	7.0222(1)	7.0147(1)
V (Å^3)	552.22(9)	551.76(8)
Formula weight	1818.58	1796.15
Calculated density (g/cm^3)	5.4667	5.4038
d Range (Å)	0.69–2.78	0.68–2.78
Number of observations	3491	3468
Number of reflections	661	668
Number of variables	55	55
R_{F2} (%)[a]	4.12	3.06
R_p (%)[a]	1.81	1.76
R_{wp} (%)[a]	2.99	2.67
R_{exp} (%)[a]	1.97	2.03

[a] See Refs. (*14, 21*).

tron sources has been reported previously (*11*).

Approximately 25 g of polycrystalline $Ca_2Nd_8(SiO_4)_6O_2$ prepared at 1250°C was divided into two samples, and each sample was sealed in a thin-walled vanadium sample tube (5 cm in length and 1.1 cm in diameter). One of the samples was subjected to ca. 423 hr of fast neutron irradiation, representing a fluence of 4.43×10^{17} n/cm^2, at the F6 horizontal beam port at IPNS in order to determine the possible effects of neutron irradiation on structure refinements. The second sample was not irradiated prior to the neutron diffraction measurements. Time-of-flight neutron powder diffraction data were collected at room temperature from both of these samples on the General Purpose Powder Diffractometer (GPPD) at IPNS under the following conditions: unirradiated sample (42.48 hr of neutrons at 30-Hz repetition rate and an average proton beam current of 7 μA) and irradiated sample (33.77 hr at 30 Hz and 7 μA). A description of the GPPD and its data acquisition system is available elsewhere (*12*).

A sample (ca. 15 g) of $Ca_{2.2}Nd_{7.8}(SiO_4)_6O_{1.9}$ (prepared at 1250°C) was sealed in a vanadium sample tube, and room-temperature powder diffraction data were also collected from this sample using the GPPD (14.50 hr at 30 Hz and 11 μA). The increase in proton beam current to 11 μA accounts for the dramatic reduction in the time needed to collect data of equivalent statistical quality to that from the $Ca_2Nd_8(SiO_4)_6O_2$ samples (see the R_{exp} values given in Table I).

Results

X-Ray Diffraction

Powder X-ray diffraction data, obtained in both the present study and the previous study (*7*), indicate the presence of a single crystalline phase for all samples in the composition range $0 \leq x \leq 4$ (not considering

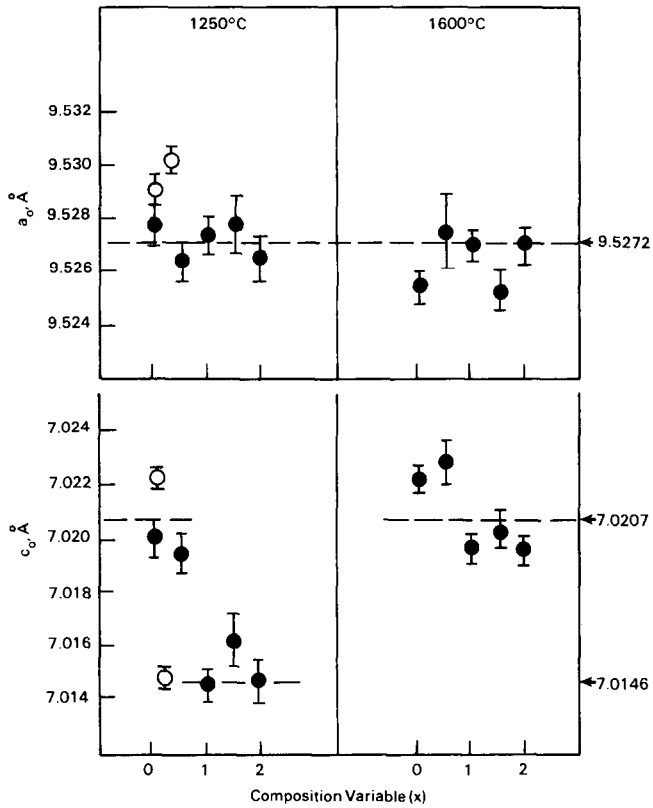

FIG. 1. The observed lattice parameters in $Ca_{2+x}Nd_{8-x}(SiO_4)_6O_{2-0.5x}$ system as a function of x and sample preparation temperature. Solid data points are from X-ray diffraction measurements; open data points are from neutron diffraction measurements.

any amorphous material which may be present). The calculated lattice parameters of this phase (in the present study) as a function of bulk composition and preparation temperature are shown in Fig. 1. The results exhibit some scatter which can be attributed to deviations from equilibrium associated with the sample cooling. However, several features of these results are apparent. There is relatively little variation in the a_0 parameter with bulk composition and preparation temperature. The c_0 parameter shows a greater degree of variation with composition, particularly at 1250°C where a significant change occurs between $x = 0$ and $x = 1$. This supports our previous conclusion (*7*) that the composition of the apatite phase in this system is limited to $x \leq 1$ at 1250°C. The variation in c_0 decreases at 1600°C, suggesting that the composition range of the apatite is even further reduced and may be approaching a limit of $x \cong 0$ at this temperature, as suggested previously (*7*).

It is necessary to postulate the presence of a second phase, in those samples with $x > 1$, to account for the material (Ca, Si, O) in the bulk composition not incorporated into the crystalline apatite phase. This secondary phase appears to be amorphous to X rays since no unaccounted peaks are present in the diffraction patterns. This is further supported by our previous observation (*7*) of a glass-like Ca–Si–O phase in

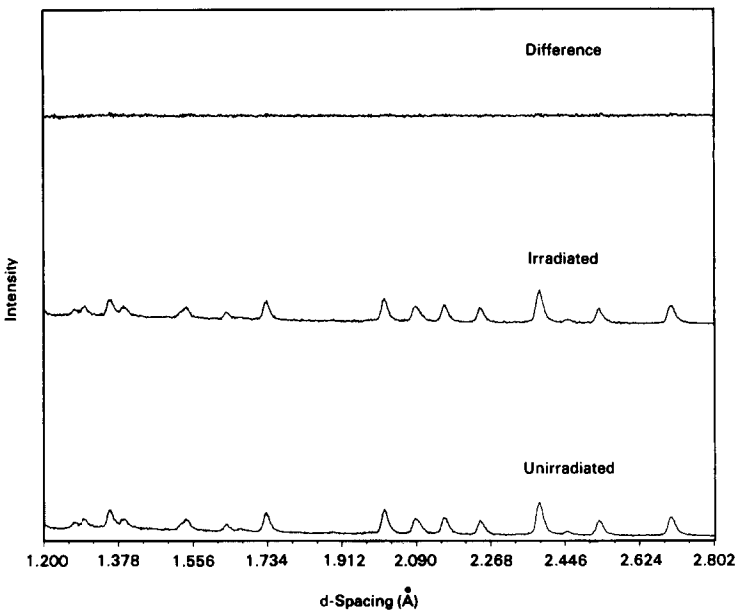

FIG. 2. Raw time-of-flight neutron powder data (GPPD; $2\theta = \pm 151°$) from the unirradiated and irradiated $Ca_2Nd_8(SiO_4)_6O_2$ samples, normalized to each other and compared (difference) over the range of d spacings from 1.2 to 2.8 Å.

samples with $x = 2$ and $x = 4$. Furthermore, no secondary phase has yet been observed in our extensive investigations of the $x = 0$ composition, which have included both analytical and high-resolution transmission electron microscopy.

Neutron Irradiation

As depicted in Fig. 2, neutron irradiation of $Ca_2Nd_8(SiO_4)_6O_2$ to a total fluence of 4.43×10^{17} n/cm^2 (>0.1 MeV) results in no discernible difference in the neutron powder diffraction spectrum. This is not too surprising since a neutron fluence of 4.43×10^{17} n/cm^2 corresponds to a relatively low displacement dose in this material of about 0.0005–0.001 dpa (displacements per atom). In a previous study of radiation damage in this material (*4*), lattice parameter changes were measured out to displacement doses on the order of 0.2 dpa, using both external irradiation with α particles and self-radiation from the α decay of incorporated ^{244}Cm. In both cases, the derived functional dependence of the structural changes with dose predict that the lattice parameter changes should be no more than 0.01% at 0.001 dpa, which is within the uncertainty of the results in Fig. 2. Consequently, no effects of the neutron irradiation (carried out at even lower doses during the neutron diffraction measurements) should be observed in the structural refinements. It should also be noted that in order to simulate (with neutrons) the higher displacement damage associated with α decay in nuclear waste materials, a fast neutron fluence between 5×10^{18} n/cm^2 and 10^{20} n/cm^2 (0.01 to 0.2 dpa) would be needed.

Neutron Diffraction

Data from the backscattering detector banks of the GPPD from the unirradiated $Ca_2Nd_8(SiO_4)_6O_2$ ($2\theta = \pm 151°$) and $Ca_{2.2}Nd_{7.8}(SiO_4)_6O_{1.9}$ ($2\theta = \pm 150°$) sam-

TABLE II

POSITIONAL AND ANISOTROPIC THERMAL ($\times 10^4$) PARAMETERS FROM RIETVELD ANALYSES FOR $Ca_{2+x}Nd_{8-x}(SiO_4)_6O_{2-0.5x}$[a,b]

Atom	Site	Occupation	x	y	z	β_{11}	β_{22}	β_{33}	β_{12}	β_{13}	β_{23}
					(a) $Ca_2Nd_8(SiO_4)_6O_2$						
Ca1	4*f*	1.79(8)	$\frac{1}{3}$	$\frac{2}{3}$	−0.0002(4)	30(2)	$=\beta_{11}$	27(4)	$=\beta_{11/2}$	0	0
Nd1		2.21(8)									
Ca2	6*h*	0.21(8)	0.2322(2)	−0.0105(2)	$\frac{1}{4}$	16(2)	12(2)	22(2)	6(2)	0	0
Nd2		5.79(8)									
Si	6*h*	6	0.4025(3)	0.3742(3)	$\frac{1}{4}$	19(4)	27(4)	27(5)	19(4)	0	0
O1	6*h*	6	0.3222(3)	0.4879(3)	$\frac{1}{4}$	64(4)	38(4)	18(4)	38(3)	0	0
O2	6*h*	6	0.5966(2)	0.4702(3)	$\frac{1}{4}$	18(3)	24(3)	75(5)	16(2)	0	0
O3	12*i*	12	0.3418(2)	0.2531(2)	0.0671(2)	97(3)	26(2)	47(3)	30(2)	−31(2)	−17(2)
O4	2*a*	2	0	0	$\frac{1}{4}$	24(3)	$=\beta_{11}$	159(9)	$=\beta_{11/2}$	0	0
					(b) $Ca_{2.2}Nd_{7.8}(SiO_4)_6O_{1.9}$						
Ca1	4*f*	1.60(4)	$\frac{1}{3}$	$\frac{2}{3}$	−0.0001(3)	34(2)	$=\beta_{11}$	39(3)	$=\beta_{11/2}$	0	0
Nd1		2.40(4)									
Ca2	6*h*	0.60(4)	0.2339(2)	−0.0109(2)	$\frac{1}{4}$	20(2)	17(2)	20(2)	7(2)	0	0
Nd2		5.40(4)									
Si	6*h*	6	0.4008(3)	0.3727(3)	$\frac{1}{4}$	28(3)	12(3)	14(4)	19(3)	0	0
O1	6*h*	6	0.3224(2)	0.4876(2)	$\frac{1}{4}$	64(3)	35(3)	27(4)	42(3)	0	0
O2	6*h*	6	0.5967(2)	0.4697(2)	$\frac{1}{4}$	13(3)	11(2)	116(5)	2(2)	0	0
O3	12*i*	12	0.3427(2)	0.2530(2)	0.0669(2)	121(3)	35(2)	31(2)	42(2)	−41(2)	−12(2)
O4	2*a*	1.90(4)	0	0	$\frac{1}{4}$	13(4)	$=\beta_{11}$	270(12)	$=\beta_{11/2}$	0	0

[a] esd's, shown in parentheses, are right-adjusted to the last digit of the preceding number, and they are derived from the inverse of the final least-squares matrix.

[b] The anisotropic thermal parameters enter the calculated structure factor expression in the form

$$\exp[-(h^2\beta_{11} + k^2\beta_{22} + l^2\beta_{33} + 2hk\beta_{12} + 2hl\beta_{13} + 2kl\beta_{23})].$$

ples were analyzed using the Rietveld method (*13, 14*) adapted for the time-of-flight technique (*15*). The initial structural parameters were taken from the previous X-ray work (*7*), and the neutron scattering lengths of Koester (*16*) for Ca, Nd, Si, and O were used. A five-parameter Chebyschev polynomial was used to model the background, and a peak shape function with a three-parameter Gaussian component, $\sigma = [\sigma_0^2 + \sigma_1^2 d^2 + \sigma_2^2 d^4]^{1/2}$, was assumed (*17*). A parameter to account for the long wavelength effects of sample absorption was refined, but neither data set was seen to suffer from preferred sample orientation or extinction. All atoms were refined with anisotropic temperature factors. The distribution of Ca and Nd over the 4*f* and 6*h* metal sites was determined by constraining the individual metal site occupations to 4 and 6, respectively, and by constricting the overall metal stoichiometry to 10; for the $Ca_{2.2}Nd_{7.8}(SiO_4)_6O_{1.9}$ refinement, the further constraint that the stoichiometry of the anionic oxygen, O4, should vary by half of the Nd stoichiometry was also assumed.

Table I summarizes the conditions and discrepancy indices from the refinements of $Ca_2Nd_8(SiO_4)_6O_2$ and $Ca_{2.2}Nd_{7.8}(SiO_4)_6O_{1.9}$; the final refined structural parameters for the two samples are collected in Table II. The raw data and the final calculated spectra based on the refined model for each of the two data sets are shown in Figs. 3 and 4.

Discussion

Selected bond distances and angles are listed in Table III for $Ca_2Nd_8(SiO_4)_6O_2$ and $Ca_{2.2}Nd_{7.8}(SiO_4)_6O_{1.9}$. The structural data for the silicate ion provides an internal standard for evaluating the refinements. The Si–O bond lengths range from 1.602(4) to 1.628(2) Å in $Ca_2Nd_8(SiO_4)_6O_2$, with an av-

TABLE III

SELECTED BOND DISTANCES (Å), ANGLES (°), AND esd's[a]

		Number[b]	$Ca_2Nd_8(SiO_4)_6O_2$	$Ca_{2.2}Nd_{7.8}(SiO_4)_6O_{1.9}$
Distances involving silicon				
Si	O1	1	1.609(3)	1.606(2)
Si	O2	1	1.602(4)	1.616(3)
Si	O3	2	1.628(2)	1.620(2)
Angles around silicon				
O1 Si	O2	1	114.7(2)	114.1(2)
O1 Si	O3	2	111.0(1)	111.6(1)
O2 Si	O3	2	107.7(1)	107.1(1)
O3 Si	O3	1	104.2(2)	104.8(2)
Distances involving Ca1/Nd1				
Ca1/Nd1	O1	3	2.412(2)	2.413(2)
Ca1/Nd1	O2	3	2.468(2)	2.464(2)
Ca1/Nd1	O3	3	2.832(2)	2.824(2)
Distances involving Ca2/Nd2				
Ca2/Nd2	O1	1	2.710(3)	2.702(2)
Ca2/Nd2	O2	1	2.459(3)	2.449(2)
Ca2/Nd2	O3	2	2.535(2)	2.538(2)
Ca2/Nd2	O3	2	2.388(2)	2.383(1)
Ca2/Nd2	O4	1	2.264(1)	2.282(1)

[a] esd's, shown in parentheses, are right-adjusted to the last digit of the preceding number and include the effects of the full positional covariance matrix and the uncertainties of the unit cell parameters. No corrections were applied for the possible effects of thermal motion.

[b] Number of interactions of this type within the coordination sphere of the specified atom.

erage value of 1.617 ± 0.013 Å, and in $Ca_{2.2}Nd_{7.8}(SiO_4)_6O_{1.9}$, the range of these distances is 1.606(2) to 1.620(2) Å, with an average value of 1.616 ± 0.007 Å.[2] These results are in excellent agreement with one another, with previous X-ray diffraction results on this system (*7*), and also with reported Si–O bond distances that range from 1.546 to 1.688 Å, with an average value of 1.63 Å, in several silicates (*18*). In addition, the average O–Si–O bond angle (109.4 ± 3.6° for both $Ca_2Nd_8(SiO_4)_6O_2$ and $Ca_{2.2}Nd_{7.8}(SiO_4)_6O_{1.9}$) is close to the ideal tetrahedral value.

[2] Esd's (σ_{mean}) quoted for average distances and angles throughout the text are given as ±X.XXX and are a measure of the scatter of the individual results from the average as calculated by

$$\sigma_{mean} = \left[\left(\sum_N (x_N - \bar{x})^{-2}\right)\Big/(N-1)\right]^{1/2}$$

where x is the average of N measurements and x_N is the Nth such measurement.

Figure 5 is an ORTEP-II drawing of the unit cell of $Ca_{2+x}Nd_{8-x}(SiO_4)_6O_{2-0.5x}$. In this structure, the silicate groups are isolated from one another and serve to link the various metal ions. Nine silicate oxygens (O1, O2, or O3) are coordinated to the metal 4*f* site (Ca1/Nd1)—three O2–O3 edges of three different SiO_4 tetrahedra acting as bidentate ligands and three O1 atoms from different silicate groups, as shown in Fig. 6a. The metal 6*h* site (Ca2/Nd2) is surrounded by six silicate oxygens (one O3–O3 bidentate ligand, one O1, one O2, and two O3) and one anionic oxygen (O4), as shown in Fig. 6b. Each silicate oxygen is coordinated to three metal ions (O1 and O2 to two metal ions in 4*f* sites and one metal ion in a 6*h* site, and O3 to one metal ion in a 4*f* site and two metal ions in 6*h* sites), while the anionic oxygen is surrounded by three metal ions occupying 6*h* sites only.

The average metal–oxygen distances in $Ca_2Nd_8(SiO_4)_6O_2$ are 2.57 ± 0.20 Å for Ca1/Nd1–O and a smaller distance of 2.47 ± 0.14 Å for Ca2/Nd2–O. For $Ca_{2.2}Nd_{7.8}(SiO_4)_6O_{1.9}$, the difference in the average distances persists with 2.57 ± 0.19 Å for Ca1/Nd1–O and 2.47 ± 0.14 Å for Ca2/Nd2–O. This variation in distances is consistent with the weighted average ionic radii for the metal ions occupying the 4*f* and 6*h* sites. Using the ionic radii of Shannon and Prewitt (*19*), corrected for coordination number, the expected distances for the two sites are 2.51 and 2.43 Å, respectively.

The metal–oxygen (Ca2/Nd2–O_4) distance [2.264(1) Å in $Ca_2Nd_8(SiO_4)_6O_2$ and 2.282(1) Å in $Ca_{2.2}Nd_{7.8}(SiO_4)_6O_{1.9}$] is considerably shorter than the sum of the ionic radii (2.44 Å) (*19*). However, similar deviations found in other rare earth apatites (*20*) have been attributed to the strong polarizing forces exerted by the rare earth cation on the anionic oxygen. The change in the

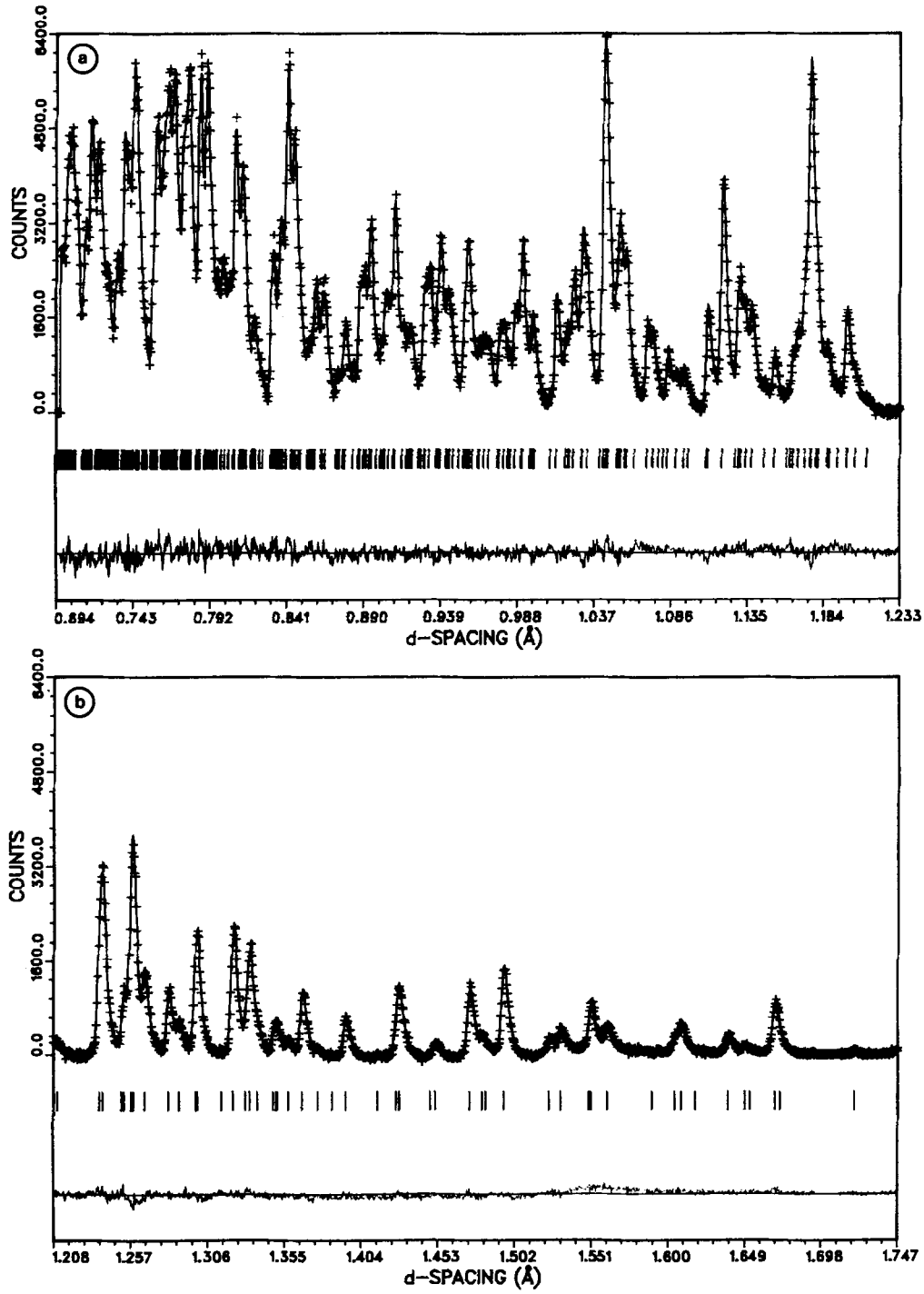

FIG. 3. (a–d) The observed neutron diffraction data (+) and fit to the data (line) from the Rietveld analysis of $Ca_2Nd_8(SiO_4)_6O_2$ (GPPD, $2\theta = \pm 151°$; hexagonal $P6_3/m$). Tick marks below the data indicate the positions of allowed Bragg reflections included in the calculation. The curve at the bottom of the figure shows the difference between the observed data and the calculation. The background has been subtracted before plotting.

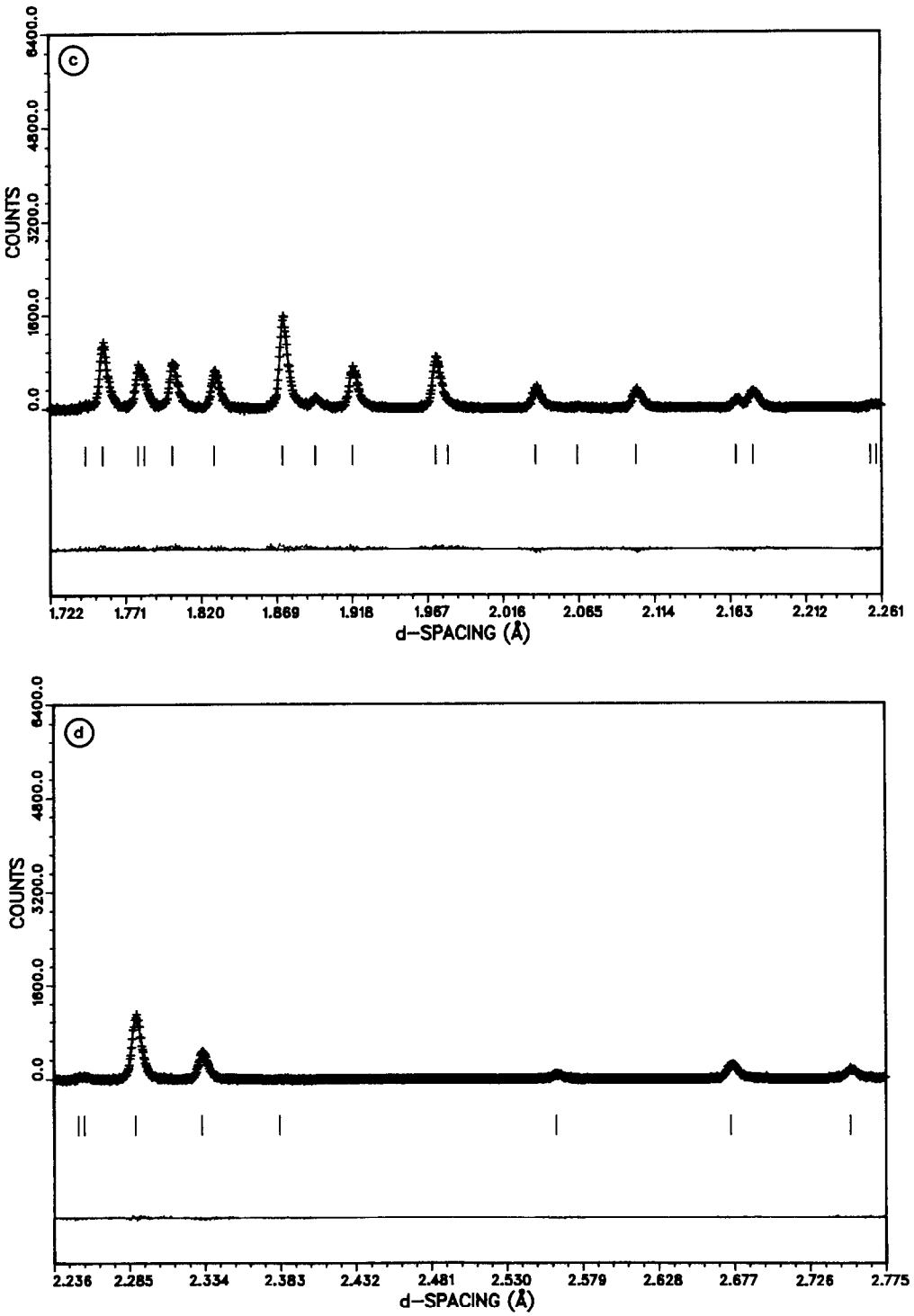

FIG. 3—*Continued.*

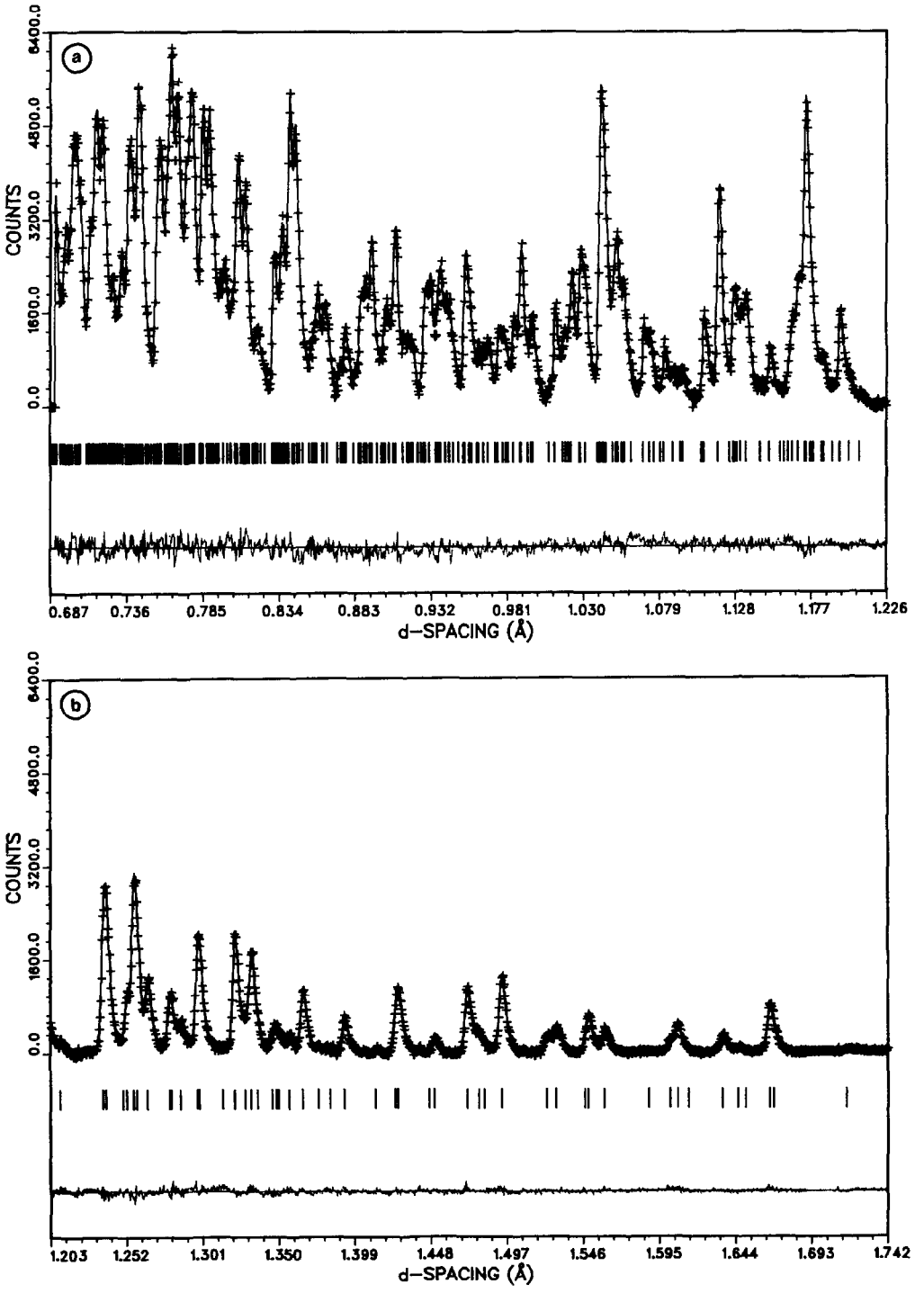

FIG. 4. (a–d) The observed neutron diffraction data (+) and fit to the data (line) from the Rietveld analysis of $Ca_{2.2}Nd_{7.8}(SiO_4)_6O_{1.9}$ (GPPD, $2\theta = \pm 150°$; hexagonal $P6_3/m$).

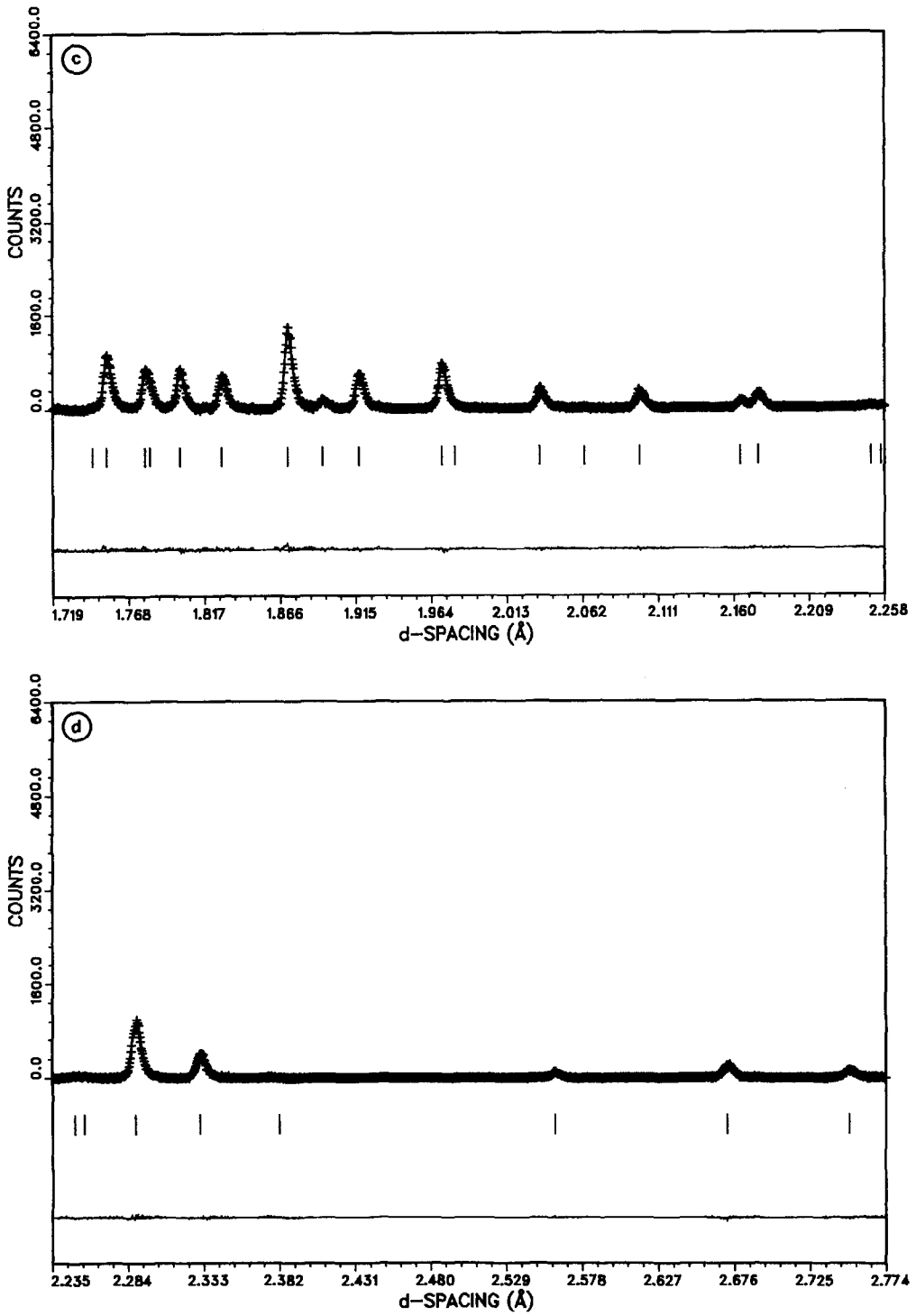

FIG. 4—*Continued.*

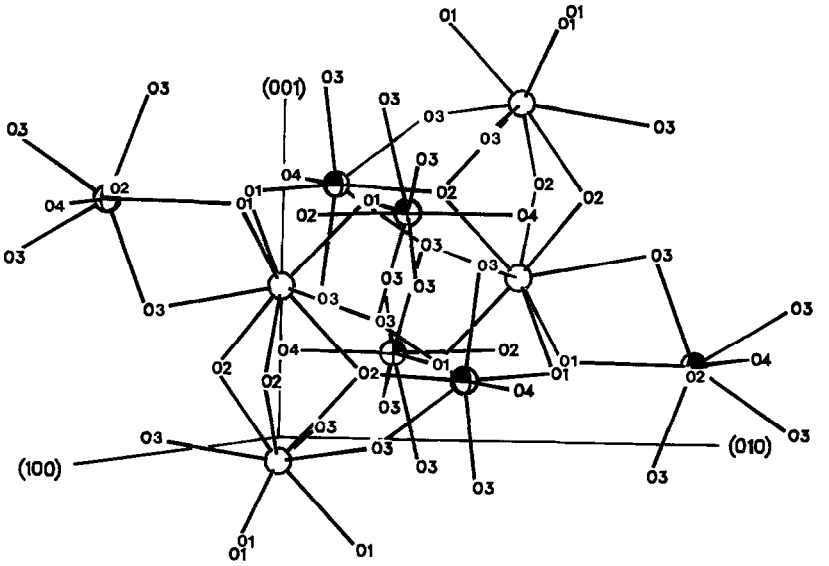

FIG. 5. The projected unit cell of $Ca_{2+x}Nd_{8-x}(SiO_4)_6O_{2-0.5x}$ viewed approximately down the a^* direction (the basal (110) plane is tilted down by 5°). The open circles represent the metal 4*f* (Ca1/Nd1) positions, and the spheres with one filled quadrant, the metal 6*h* (Ca2/Nd2) positions. All silicon atoms and silicate oxygens that do not link metal positions have been omitted.

metal–oxygen (Ca2/Nd2–O4) distance with composition can be explained in terms of the increased cation repulsion associated with the partially vacant anionic oxygen site in $Ca_{2.2}Nd_{7.8}(SiO_4)_6O_{1.9}$.

The metal ion distribution between the 4*f* and 6*h* sites for the two samples prepared at 1250°C ($Ca_2Nd_8(SiO_4)_6O_2$ and $Ca_{2.2}Nd_{7.8}(SiO_4)_6O_{1.9}$) may be described, respectively, as

$$(Ca_{1.79}Nd_{2.21})^{[9]}(Ca_{0.21}Nd_{5.79})^{[7]}(SiO_4)_6^{[4]}O_2^{[3]}$$

$$(Ca_{1.60}Nd_{2.40})^{[9]}(Ca_{0.60}Nd_{5.40})^{[7]}(SiO_4)_6^{[4]}O_{1.9}^{[3]}.$$

Numbers in brackets at the upper right of the elements give the coordination numbers

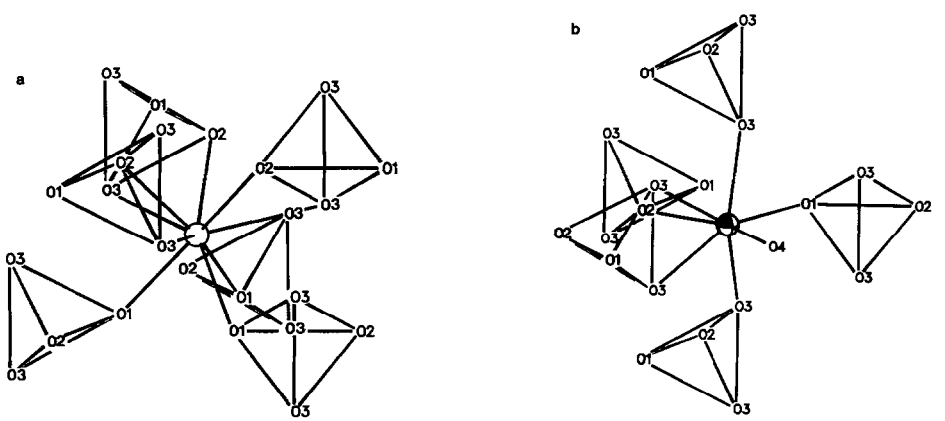

FIG. 6. The coordination spheres of the metal atom positions in $Ca_{2+x}Nd_{8-x}(SiO_4)_6O_{2-0.5x}$. Silicate groups are shown as the tetrahedra described by their oxygen atoms; silicon atoms have been omitted. (a) The metal 4*f* (Ca1/Nd1) site. (b) The metal 6*h* (Ca2/Nd2) site.

of the elements, while the subscripts give the stoichiometry and distribution of the metal ions between the 4*f* and 6*h* sites, respectively.

From this description, it is clear that, for samples prepared at 1250°C, the majority of the calcium (89% for $Ca_2Nd_8(SiO_4)_6O_2$ and 73% for $Ca_{2.2}Nd_{7.8}(SiO_4)_6O_{1.9}$) is concentrated in the nine-coordinated (4*f*) site. This represents a strong ordering of the calcium ions relative to a random distribution in which only 40% of the calcium would occupy the 4*f* site. The reduced ordering in $Ca_{2.2}Nd_{7.8}(SiO_4)_6O_{1.9}$ is marked by an increased concentration of calcium in the 6*h* site thereby reducing the number of Nd^{3+} ions in contact with the partially (5%) vacant anionic oxygen site (2*a*). This association of excess Ca^{2+} and vacancies in the 2*a* site will tend to compensate somewhat for the repulsive forces associated with anionic vacancies. At increasing temperatures, a much more random distribution of cations between the 4*f* and 6*h* sites is expected. This will reduce the solubility of calcium in this system, since fewer ordered 6*h* sites are available to accommodate the excess Ca^{2+}. The absence of any significant variation in the lattice parameters (Fig. 1) for the samples prepared at 1600°C suggests that the solubility of calcium is approaching the limit of $x = 0$ at this temperature and that the distribution of cations between the 4*f* and 6*h* sites is approaching a near random condition. The solubility limits of $x \cong 0$ at 1600°C and $x \cong 0.2$ at 1250°C have been estimated using unquenched samples and may not represent the true equilibrium solubility limits. However, it is clear from these data that the solubility of calcium in this structure is considerably less than previously assumed and that the oxygen-deficient structures, $x = 2$ to 4, do not exist at 1600°C.

Acknowledgments

The authors are indebted to D. E. Cox of Brookhaven National Laboratory for his advice and assistance and to G. D. Maupin (Pacific Northwest Laboratory) for assistance in sample preparation. We also with to thank members of Argonne National Laboratory who assisted in the neutron measurements: A. W. Schulke and D. E. Bohringer for neutron irradiation, as well as J. Faber, Jr., R. L. Hitterman, and M. H. Mueller for collection of the neutron diffraction data.

References

1. W. J. Weber, R. P. Turcotte, L. R. Bunnell, F. P. Roberts, and J. H. Westsik, Jr., *in* "Ceramics in Nuclear Waste Management" (T. D. Chikalla and J. E. Mendel, Eds.), pp. 294–299, CONF-790420, National Technical Information Service, Springfield, Va. (1979).
2. G. J. McCarthy, J. G. Pepin, D. E. Pfoertsch, and D. G. Clarke, *in* "Ceramics in Nuclear Waste Management" (T. D. Chikalla and J. E. Mendel, Eds.), pp. 315–320, CONF-790420, National Technical Information Service, Springfield, Va. (1979).
3. R. P. Turcotte, J. W. Wald, F. P. Roberts, J. M. Rusin, and W. Lutze, *J. Amer. Ceram. Soc.* **65,** 589 (1982).
4. W. J. Weber, *J. Amer. Ceram. Soc.* **65,** 544 (1982).
5. W. J. Weber, *Radiat. Eff.* **77,** 295 (1983).
6. G. J. McCarthy, *in* "Proceedings of the 12th Rare-Earth Research Conference" (C. E. Lundin, Ed.), Vol. II, pp. 665–676, Denver Research Institute (1976).
7. J. A. Fahey and W. J. Weber, *in* "The Rare Earths in Modern Science and Technology" (G. J. McCarthy, H. E. Silber, and J. J. Rhyne, Eds.), Vol. 3, pp. 341–344, Plenum, New York (1982).
8. A. W. Hewat, UK Atomic Energy Authority Research Group Report RRL 73/897, AERE Harwell, Oxfordshire, England (1973).
9. D. McConnell, "Apatite," Chap. 4, Springer-Verlag, New York (1973).
10. D. E. Williams, Ames Lab. Rep. IS–1052, 1964.
11. B. S. Brown, J. M. Carpenter, J. D. Jorgensen, D. L. Price, and W. A. Kamitakahara, *in* "Novel Materials and Techniques in Condensed Matter" (G. W. Crabtree and P. Vashishta, Eds.), pp. 311–340, Elsevier North-Holland, Amsterdam (1982).
12. J. D. Jorgensen and J. Faber, Jr., *in* "Proceedings of the 6th Meeting of the International Collaboration of Advanced Neutron Sources" (J. M. Carpenter, Ed.), pp. 105–114, Argonne National Laboratory, Argonne, Ill., June 28–July 2, 1982 (ANL–82–80).

13. H. M. RIETVELD, *Acta Crystallogr.* **22,** 151 (1967).
14. H. M. RIETVELD, *J. Appl. Crystallogr.* **2,** 65, (1969).
15. R. B. VON DREELE, J. D. JORGENSEN, AND C. G. WINDSOR, *J. Appl. Crystallogr.* **15,** 581 (1982).
16. L. KOESTER "Springer Tracts in Modern Physics," Vol. 80, pp. 34–41, Springer-Verlag, New York/Berlin (1977).
17. R. B. VON DREELE, personal communication.
18. D. W. J. CRUICKSHANK, *J. Chem. Soc.,* 5486 (1961).
19. R. D. SHANNON AND C. T. PREWITT, *Acta Crystallogr. B* **25,** 925 (1969).
20. J. FELSCH, *J. Solid State Chem.* **5,** 266 (1972).
21. J. D. JORGENSEN AND F. J. ROTELLA, *J. Appl. Crystallogr.* **15,** 27 (1982).